Available online at www.sciencedirect.com
SCIENCE DIRECT
Journal of Solid State Chemistry 179 (2006) 2231–2236
JOURNAL OF SOLID STATE CHEMISTRY
www.elsevier.com/locate/jssc

Structural and magnetic properties of high-pressure/high-temperature synthesized $(Sr_{1-x}R_x)CoO_3$ (R = Y and Ho) perovskites

S. Balamurugan*, E. Takayama-Muromachi

Superconducting Materials Center, National Institute for Materials Science (NIMS), 1-1 Namiki, Tsukuba, Ibaraki 305-0044, Japan

Received 9 December 2005; received in revised form 27 March 2006; accepted 24 April 2006
Available online 4 May 2006

Abstract

Polycrystalline perovskite cobalt oxides $Sr_{1-x}R_xCoO_3$ (R = Y and Ho; $0 \leqslant x \leqslant 1$) were prepared by high-pressure/high-temperature technique. X-ray powder patterns of the Y-system indicated cubic perovskite form for $0 \leqslant x \leqslant 0.5$, and orthorhombic perovskite form for $x = 0.8$ and 1.0, while coexisting of the two phases for $x = 0.6$. The cubic perovskite samples had metallic electric resistivities while the orthorhombic ones with semiconducting or insulating nature. The parent compound $SrCoO_3$ showed a ferromagnetic transition at 266 K. With the Y substitution, the transition temperature increased slightly to ~275 K at $x = 0.1$, then decreased rapidly to ~60 K for $x = 0.6$. The $YCoO_3$ ($x = 1$) sample showed non-magnetic behavior. The Ho-substituted system showed quite similar structural, transport and magnetic properties to those of the Y-system.

Keywords: Perovskite; $SrCoO_3$; $YCoO_3$; $HoCoO_3$; High-pressure synthesis; Ferromagnetism

1. Introduction

The spin state and electron configuration of the perovskite cobalt oxide $SrCoO_3$ and its related systems have been subject matter of various investigations and disputes over the past few decades. It is well known that energy difference between the low-spin (LS) state and high-spin (HS) or intermediate-spin (IS) state is quite small for both Co^{3+} and Co^{4+} due to the closeness of the crystal field splitting and the exchange energy (*Hund's rule* coupling) in the octahedral coordination. $SrCoO_{3-\delta}$ crystallizes in various structures depending on the oxygen content [1–5]. $SrCoO_{3-\delta}$ ($\delta = 0.5$) adopts a brownmillerite structure with an orthorhombic lattice of $a \approx c \approx \sqrt{2}a_p$ and $b \approx 4a_p$ regarding the cubic perovskite lattice of a_p, and is an antiferromagnet with a Néel temperature of ~570 K [3]. With decreasing oxygen deficiency ($\delta \to 0$), the compound is transformed to a cubic perovskite form via a pseudo-cubic form having a tetragonal superlattice of $a \approx 2\sqrt{2}a_p$ and $c \approx 2a_p$ [5]. The cubic (or pseudo-cubic) form of compound shows ferromagnetism with a Curie temperature (T_c) of ~220 K [6,7]. Taguchi et al. [7] investigated the crystallographic and magnetic properties of cubic (pseudo-cubic) perovskite $SrCoO_{3-\delta}$ ($\delta = 0.05-0.26$) synthesized under high-oxygen pressure, to find the systematic increase of T_c with decreasing δ. They claimed that the Co^{4+} ion was mainly in the LS state but some of the t_{2g} electrons were transferred into the e_g band. Since then, various results have been reported and most of them have supported that the Co^{4+} ion is in the LS state [6–11]. Recently, however, several groups suggested the possibility of IS state for Co^{4+} [12,13].

Rare-earth substituted systems of (Sr, R)$CoO_{3-\delta}$ (R: rare earth element) have been also studied intensively. Although studies have been rather focused on the R = La system [14–20], other systems with smaller rare-earth elements are also attracting keen interest recently. For instance, a new type of oxygen-deficient perovskite structure has been reported for $Sr_{1-x}Ln_xCoO_{3-\delta}$ (Ln = Y, Ho and Dy, x~0.3) systems [21–26]. The phase is brownmillerite like, associated with oxygen vacancy ordering and A-site cation ordering. Though its fundamental structure is described by

*Corresponding author. Fax: +81 29 860 4674.
E-mail address: sarkarainadar.balamurugan@nims.go.jp (S. Balamurugan).

0022-4596/$ - see front matter © 2006 Elsevier Inc. All rights reserved.
doi:10.1016/j.jssc.2006.04.028

tetragonal system with $I4/mmm$ and $a \approx 2a_p$ and $c \approx 4a_p$, the real structure is more complicated with a larger superlattice. Very recently, it has been found that $Sr_{1-x}Y_xCoO_{3-\delta}$ is a room temperature ferromagnet with a Curie temperature (T_c) of 335 K in a very narrow range of the Y content, $0.2 \leqslant x \leqslant 0.25$ [27].

In the previous study [28], we successfully synthesized cubic perovskite cobalt oxides $Sr_{1-x}Ca_xCoO_3$ ($0 \leqslant x \leqslant 0.8$) under high-pressure (HP) and they showed mixing of LS and HS or IS states for the Co^{4+} ion. We found that HP synthesis is quite effective to prepare Co-perovskite oxides with smaller A-site cations and without oxygen defects. The purpose of the present study is to carry out A-site substitutions by Y and Ho, and to elucidate substitution effects on the structural, magnetic, transport properties and the spin states of the cobalt ions for the perovskite cobalt oxide $SrCoO_3$. We expect that physical properties for the perovskite type oxides prepared under HP are different from those for the ambient-pressure brownmillerite-like oxides.

2. Experimental details

The polycrystalline samples of $Sr_{1-x}R_xCoO_3$ (R = Y and Ho; $x = 0-1$) were synthesized by HP/high-temperature (HT) (HP–HT) technique. The starting materials used were high purity (>3 N) fine powders of SrO_2, Co, Co_3O_4, Y_2O_3, Ho_2O_3 and $KClO_4$ (oxidizing agent). They were thoroughly mixed and ground in an agate mortar with pestle in a glove box. The oxygen content was exactly adjusted to 3.0 in the starting mixture and we needed to add $KClO_4$ for that purpose for the samples with $x \geqslant 0.8$. Approximately 250 mg of each mixture was put into an Au or Pt capsule and sealed. The sealed capsule was then allowed to react in a flat belt type HP and HT apparatus at 6 GPa and 1450–1650 °C for 2–5 h then quenched to room temperature followed by releasing of pressure. The weight of the capsule was measured before and after the HP run. The weight change was less than ~0.3 mg against total weight of 1 g of capsule (plus sample). To check the preservation of the net oxygen content and oxygen stoichiometry, we prepared $SrCoO_y$ perovskite samples with changing the y value between 2.6 and 3.8 under 6 GPa and 1450 °C and they were measured by thermogravimetry (TG).

The structure and phase purity of the HP synthesized samples were examined by powder X-ray diffraction (XRD) performed on a diffractometer (Rigaku RINT2200HF-Ultima) using the Ni-filtered Cu$K\alpha$ radiation. TG of the $SrCoO_y$ ($2.6 \leqslant y \leqslant 3.8$) samples was carried out with a Perkin-Elmer Thermogravimetric Analyzer. The samples were reduced under a 3% hydrogen/argon mixed gas over a temperature range of 30–800 °C at a heating rate 2 °C/min. Each of the samples studied decomposed under hydrogen reduction to give the component oxide SrO as well as Co metal. The measured mass loss was then used to determine the net oxygen present in the sample. The magnetic properties of the $Sr_{1-x}R_xCoO_3$ samples were measured using a commercial magnetometer with the superconducting quantum interference device (MPMS–XL, Quantum Design). The transport and magneto-transport measurements were carried out in a commercial apparatus (PPMS–6600, Quantum Design) between 5 and 320 K in magnetic fields up to 70 kOe.

3. Results and discussion

The XRD patterns of the HP synthesized $Sr_{1-x}Y_xCoO_3$ ($0 \leqslant x \leqslant 1$) samples are shown in Fig. 1(a). For $0 \leqslant x \leqslant 0.5$, the XRD patterns could be indexed on the basis of cubic perovskite structure and the lattice parameters decreased with increasing x consistent with a smaller ionic radius of Y^{3+} than that of Sr^{2+}. On the other hand, the XRD patterns for $x = 0.8$ and 1.0 were indexed by the orthorhombic structure except a few weak peaks of KCl

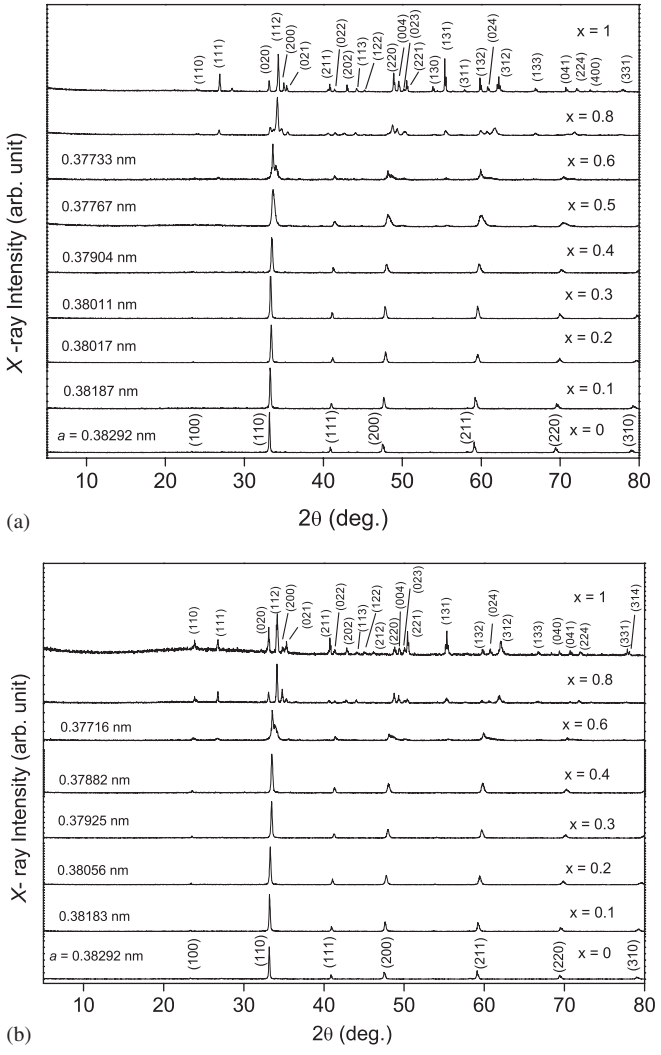

Fig. 1. (a) XRD patterns of the $Sr_{1-x}Y_xCoO_3$ system. The data shown are the lattice parameters of the cubic perovskite phases. (b) XRD patterns of the $Sr_{1-x}Ho_xCoO_3$ system. The data shown are the lattice parameters of the cubic perovskite phases.

(which was formed from $KClO_4$ used as the oxidizer). These weak peaks of KCl can be seen only in the enlarged form of XRD patterns. The calculated lattice parameters for $x = 1.0$ ($a = 0.51322$ nm; $b = 0.54106$ nm; $c = 0.73602$ nm) are slightly smaller than but in agreement with those reported for the (distorted) perovskite $YCoO_3$ [29–31]. For $x = 0.6$, the XRD pattern consists of superposition of the cubic and orthorhombic patterns indicating the two-phase coexisting region of cubic and orthorhombic perovskites.

The XRD patterns of the $Sr_{1-x}Ho_xCoO_3$ ($0 \leqslant x \leqslant 1$) samples are shown in Fig. 1(b), which is quite similar to Fig. 1(a). For $0 \leqslant x \leqslant 0.4$, the XRD patterns were indexed by the cubic system with the lattice parameter increasing with the x-value while those for $x = 0.8$ and 1.0 were by the orthorhombic system. A few weak peaks of KCl (similar to that of the Y-system) was seen in the XRD patterns of $x = 0.8$ and 1.0 samples. The calculated lattice parameters for $HoCoO_3$ ($x = 1$) ($a = 0.51271$ nm; $b = 0.53981$ nm; $c = 0.73479$ nm) are slightly smaller than but in agreement with those in the previous reports [29,32]. The XRD pattern for $x = 0.6$ can be indexed assuming mixing of the cubic and orthorhombic structures indicating the two-phase coexisting region.

In order to check the net oxygen content and oxygen stoichiometry, the $SrCoO_y$ ($2.6 \leqslant y \leqslant 3.8$) perovskite samples were analyzed by TG. The TG analysis shows that the net oxygen content was maintained in the HP process being close to the nominal value (see Fig. 2). On the other hand, lattice parameter of the $SrCoO_y$ first decreased with increasing y then had an almost constant value for $y \geqslant 3.0$ indicating the maximum limit of oxygen content in the perovskite phase to be 3.0. The remaining oxygen atoms may be concentrated in impurity phase(s) though it was not detected by XRD. Thus oxygen stoichiometry of 3.0 was realized by the nominal oxygen content of 3.0 in $SrCoO_y$ in spite of the fact that oxygen deficiency tends to be introduced easier in a Sr-richer phase. From these results, we concluded that the present series of samples had oxygen stoichiometry close to 3.0 because their nominal oxygen contents had been adjusted to 3.0. The detailed results of the $SrCoO_y$ perovsikite phases will be reported elsewhere [33].

Figs. 3(a) and (b) shows the temperature dependence of electrical resistivity, ρ for the $Sr_{1-x}R_xCoO_3$ with R = Y and Ho systems, respectively. In both systems, the sample within the cubic perovskite region ($0 \leqslant x \leqslant \sim 0.5$) had metallic electric resistivity with a positive temperature dependence (except for slight upturn in low-temperature region seen in some cases). With the substitution of Y or Ho for Sr, the Co valence decreases from 4+ for $x = 0$ to

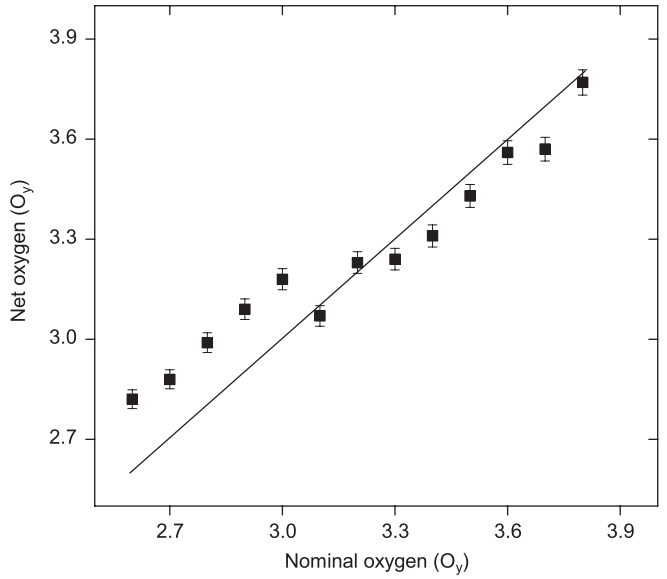

Fig. 2. TGA data for the $SrCoO_y$ perovskite samples with $2.6 \leqslant y \leqslant 3.8$.

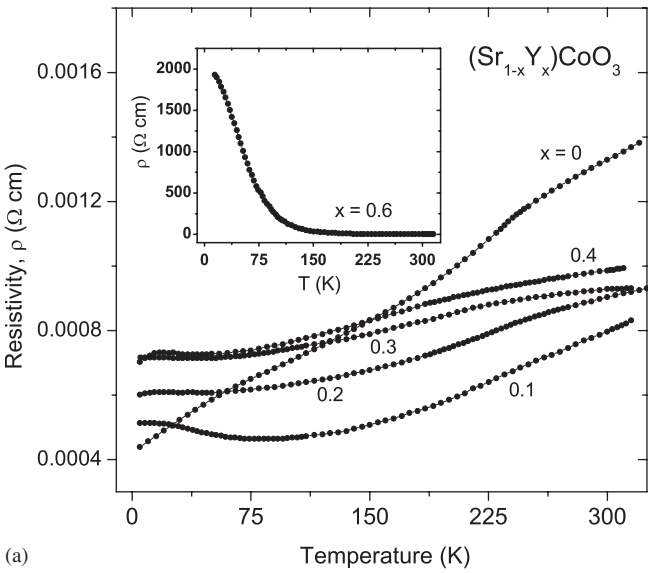

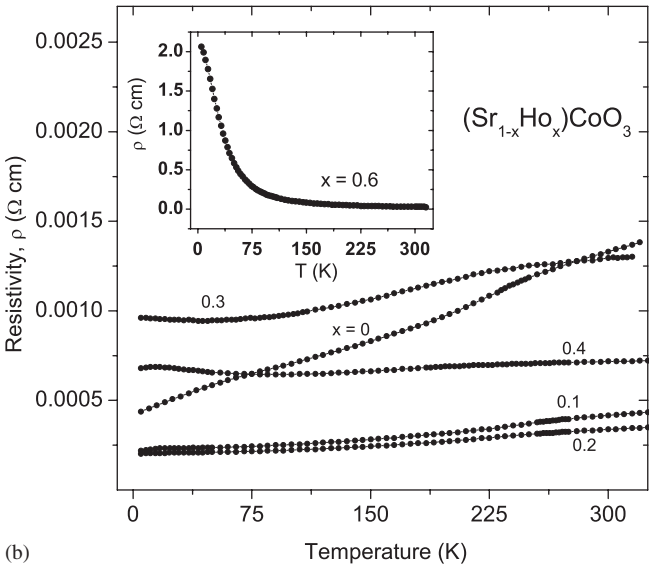

Fig. 3. (a) Temperature dependence of electrical resistivity, ρ of the $Sr_{1-x}Y_xCoO_3$ system. Inset shows the data for the $x = 0.6$ sample. (b) Temperature dependence of electrical resistivity, ρ of the $Sr_{1-x}Ho_xCoO_3$ system. Inset shows data for the $x = 0.6$ sample.

3+ for $x = 1.0$, i.e., electrons (carriers) are doped by the substitution. For the cubic perovskite samples of the both systems, room temperature resistivity decreases significantly with the substitution up to $x \sim 0.2$ then increases for higher substitution. The first decrease may reflect the enhancement of the carrier density by the substitution while the increase after further substitution may be caused by the introduction of randomness accompanying the substitution. In addition, temperature dependence of resistivity becomes less pronounced with the substitution with upturn in low-temperature range in some cases. This may be also caused by the low-temperature localization of carriers due to the random potentials introduced by the substitution.

The $x = 0.6$ samples of both systems which were the mixtures of the cubic and orthorhombic perovskite phases showed semiconducting behaviors with very high resistivities at low temperature. In the both systems, the resistivities for $x = 0.8$ and 1.0 were too high at low temperatures to be measured by our measuring system. The orthorhombic perovskites of $YCoO_3$ [29,30] and $HoCoO_3$ [29,32] have been reported to have semiconducting (or insulating in low-temperature region) nature. The mixing of the orthorhombic phase caused the high resistivity of each $x = 0.6$ sample. (The higher resistivities of the $x = 0.8$ and 1.0 compositions may be partly due to the presence of KCl at the grain-boundaries as well as the changes in the electronic structure by replacing R for Sr.)

We reported previously that $SrCoO_3$ showed a relatively large (~5.5%) negative magnetoresistance in the vicinity of the ferromagnetic transition temperature [28]. To test the substitution effects of Y and Ho on the magnetoresistance, electric resistivity under a magnetic field of 70 kOe was measured for $Sr_{1-x}R_xCoO_3$. Negative magnetoresistance similar to that of $SrCoO_3$ was observed in the substituted systems but it became less pronounced with increasing x.

Fig. 4 shows M/H (M: magnetization, H: magnetic field) plotted against temperature for the $Sr_{1-x}Y_xCoO_3$ system at an applied magnetic field of 1 kOe in the field-cooling condition. The $SrCoO_3$ perovskite undergoes ferromagnetic transition with Curie temperature depending on oxygen deficiency; our sample prepared from stoichiometric starting composition under HP had T_c ~266 K [28]. For the Y-substituted system, T_c increased slightly to ~275 K at $x = 0.1$, then decreased rapidly to ~60 K for $x = 0.6$. For $x = 0.8$, ferromagnetism disappeared almost completely. The end member of $YCoO_3$ showed no spontaneous magnetization.

The magnetic hysteresis (M–H) curves were measured at 1.8 K for the $Sr_{1-x}Y_xCoO_3$ samples and are depicted in Fig. 5. $SrCoO_3$ showed a very narrow magnetic hysteresis loop with a small coercive field (H_c) of 0.07 kOe. With increasing x, the coercive field increased to 8.3 kOe for $x = 0.6$ (Table 1) indicating that magnetic anisotropy energy increases with the Y substitution (up to $x = 0.6$). Saturation magnetization, M_s of the system was obtained from extrapolation of high magnetic field ($H > 4.5$ T) magnetization data to zero field. The M_s was 1.76 μ_B/Co atom for $x = 0$ and altered with increasing $x = 0.2$ then decreased steeply with increasing x.

The field cooled magnetization of the Y-substituted system was measured above T_c at a high applied magnetic field of 2 kOe to obtain the inverse molar magnetic susceptibility, χ^{-1} as shown in Fig. 6. It is seen that the inverse susceptibility obeys Curie–Weiss law, $\chi^{-1} = C/(T-\Theta)$, where C is Curie constant and Θ is Curie–Weiss temperature. From the Curie constant, the effective number of Bohr magnetons P_{eff} was calculated, and then, the spin S was estimated according to $P_{eff} = g\sqrt{S(S+1)}$ assuming that the g-factor was equal to 2 (spin-only moment). The Θ, P_{eff}, S thus obtained are listed in Table 1.

Firstly, we will discuss the magnetic data of the Y-based cubic perovskite samples. The Co oxidation state of $SrCoO_3$ is 4+, and based on ionic model, $S = 1/2$, 3/2 and 5/2 are expected for the LS (t_{2g}^5), IS ($t_{2g}^4 e_g^1$) and HS

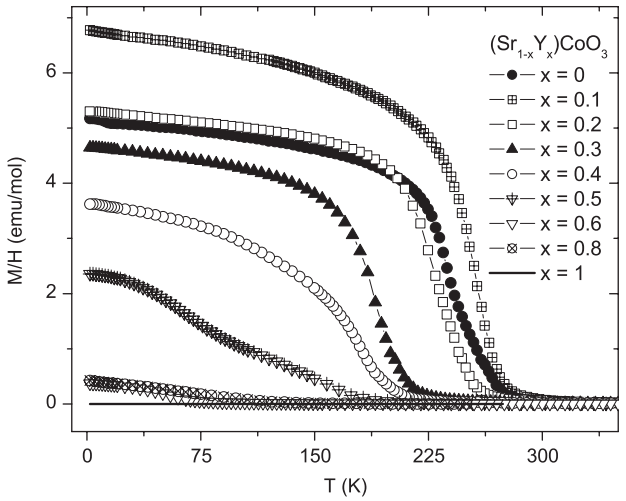

Fig. 4. Temperature dependence of M/H for the $Sr_{1-x}Y_xCoO_3$ system measured at an applied field of 1 kOe by the field-cooling mode.

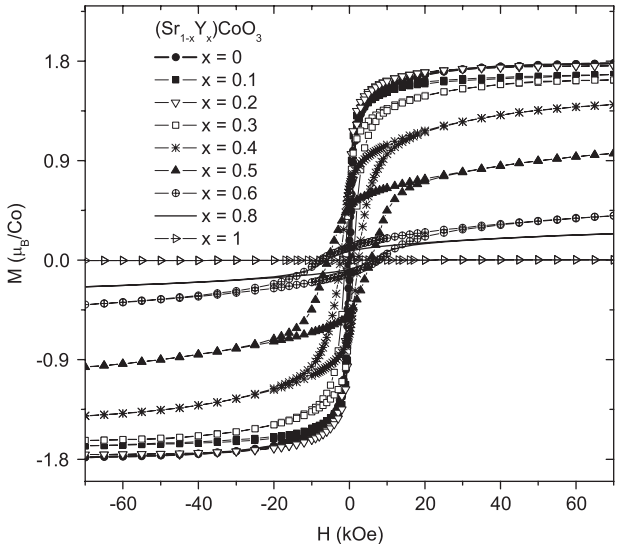

Fig. 5. Magnetic hysteresis curves for the $Sr_{1-x}Y_xCoO_3$ system generated at 1.8 K.

Table 1
Composition (x), Curie temperature (T_c), Curie–Weiss temperature (Θ), effective number of Bohr magnetons (P_{eff}), saturation magnetization (M_s), coercive field (H_c) at 1.8 K, spin (S) and $2S/M_s$ value for the $Sr_{1-x}Y_xCoO_3$ system

x	T_c (± 2 K)	Θ (K)	P_{eff} (μ_B/Co)	M_s (μ_B/Co)	H_c (kOe)	S	$2S/M_s$
0	266 (266)[a]	263.6	3.17	1.76	0.07	1.16	1.32
0.1	275 (270)	252.20	3.20	1.66	0.32	1.17	1.41
0.2	260 (260)	257.43	3.27	1.75	0.44	1.21	1.38
0.3	220 (230)	236.04	3.29	1.62	1.18	1.22	1.51
0.4	205 (200)	220.88	3.14	1.36	2.4	1.15	1.69
0.5	175	178.50	2.75	0.88	5.67	0.96	2.18
0.6	65 (60)	7.38[b]	2.93[b]	0.34[b]	8.3[b]	1.05[b]	6.17[b]

[a] T_c in the parentheses is for $Sr_{1-x}Ho_xCoO_3$.
[b] Not corrected for the mixing of the orthorhombic perovskite phase.

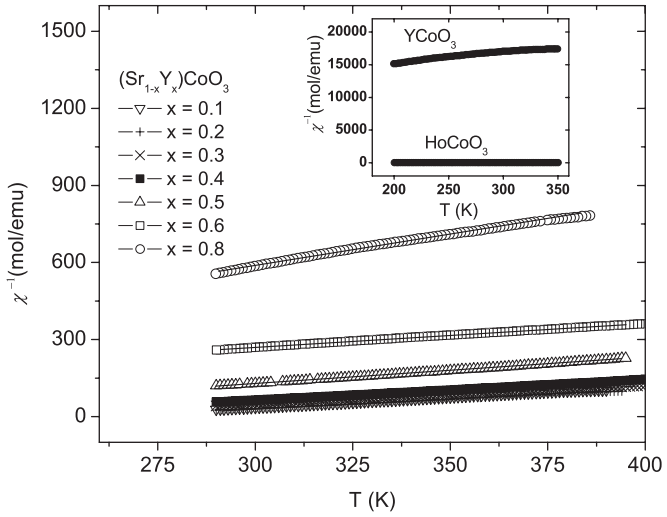

Fig. 6. Temperature dependence of inverse molar magnetic susceptibility, χ^{-1} for the $Sr_{1-x}Y_xCoO_3$ system. Susceptibilities were measured under an applied magnetic field of 2 kOe in the field-cooling mode. The inset shows the data for the $YCoO_3$ and $HoCoO_3$ samples. The solid line represents the Curie–Weiss fit.

($t_{2g}^3e_g^2$) state of Co^{4+}. As stated previously [28], the experimental value is close to $S=1$ and it is safely concluded that some of d electrons are introduced into the e_g states (bands) because the t_{2g}^5 configuration gives $S=1/2$ at most even when it is fully polarized. The S-value close to 1 suggests $t_{2g}^4e_g^1$-like configuration with localized t_{2g} electrons, and itinerant and depolarized e_g electrons [28]. With the Y substitution, electrons are doped into the system, but the S-value was kept almost constant being close to 1 for the cubic perovskite region (up to $x=0.6$, though the $x=0.6$ sample contained the orthorhombic perovskite as the minor phase). This fact suggests a picture that doped electrons by the Y substitution are introduced into the e_g bands forming $t_{2g}^4e_g^{1+x}$-like (IS-like) configuration with localized t_{2g} electrons and itinerant (and depolarized) e_g electrons.

Aforementioned picture implies the Zener's double exchange model [34] for the ferromagnetically ordered state below T_c, i.e., the itinerant (e_g) electrons couple the Co (t_{2g}) moments ferromagnetically when their spins are conserved during transport. If we assume full polarization for the e_g electrons below T_c based on this model, we expect $3+x\,\mu_B$/Co atom for the saturation magnetization M_s. Actual M_s is always much smaller than this value and tends to decrease with x as seen in Table 1. This fact suggests transfer of the electrons from e_g to t_{2g} states below T_c, i.e., mixing of the LS (t_{2g}^5)-like configuration in low-temperature region. The tendency of decreasing of M_s with x may reflect that such transfer is more pronounced in a Y-rich phase. We reported [28] similar behavior for the ferromagnetic system of $Sr_{1-x}Ca_xCoO_3$ in which M_s is smaller than $3\,\mu_B$/Co atom and tend to decrease with x, though the Co oxidation state of this system was kept constant to be 4+ different from the present case. According to the decrease of the perovskite cubic cell parameter as x increases, the orbital hybridization of the neighboring Co and O would change along the solid solution. This effect may be taken into account and the simple e_g/t_{2g} orbital filling model may not be enough for explaining the magnetism of the present system. On the other hand, for the $Sr_{1-x}Ca_xCoO_3$ system [28], we suggested itinerant-electron ferromagnetism picture as a possibility other than the double exchange like picture, because the simple relation of $2S=M_s$ was not applicable but $2S/M_s$ had a value of 1.2–1.9 implying the Rhodes–Wohlfarth relationship [35]. As shown in Table 1, the present system also has $2S/M_s$ which is larger than unity and increases with decreasing T_c remaining the possibility of the itinerant-electron ferromagnetism picture for the cubic perovskite of $Sr_{1-x}Y_xCoO_3$.

The orthorhombic $YCoO_3$ showed non-magnetic behavior under low temperature as shown in Fig. 5 indicating the LS state for the Co^{3+} ion. The Curie–Weiss fit for the magnetic data around 300 K (see Fig. 6) gave apparent values of P_{eff} and Θ to be $0.79\,\mu_B$/Co atom ($S=0.14$) and -996.3 K, respectively. This result also suggests the non-magnetic LS state for the Co^{3+} ion around 300 K.

We obtained M–H curves and χ^{-1} plots for the $Sr_{1-x}Ho_xCoO_3$ system as well as for the $Sr_{1-x}Y_xCoO_3$ system. However, we can say only little from the magnetic data of $Sr_{1-x}Ho_xCoO_3$ system because very large Ho moment ($P_{eff}=10.58\,\mu_B$/Co atom) hided the Co moment. For instance, χ^{-1} plot for $HoCoO_3$ in a range around room

temperature gave a P_{eff} value of 10.29 μ_B/Co atom. This value is close to (even smaller than) that of the Ho^{3+} ion, and thus any information on the Co moment was not obtained from this datum. The M–H curve of $HoCoO_3$, on the other hand, gave $M = 5.4\,\mu_B$/molecule at 1.8 K and 70 kOe. If the Ho moment is completely saturated, we expect $M = 10\,\mu_B$/Ho atom, and thus the Ho moment in $HoCoO_3$ was not saturated even at 1.8 K and 70 kOe probably due to antiferromagnetic interaction between the Ho moments. This means again that we cannot draw any information on the Co moment from the low-temperature magnetization data. From the lattice parameter variation and T_c variation (see Table 1) as functions of x in $Sr_{1-x}Ho_xCoO_3$ very similar to those of $Sr_{1-x}Y_xCoO_3$, we expect that essentially the same mechanism governs the ferromagnetism of the both systems.

4. Conclusion

The structural, magnetic and the transport properties of HP–HT synthesized polycrystalline $Sr_{1-x}R_xCoO_3$ ($R = Y$ or Ho; $0 \leqslant x \leqslant 1$) samples have been investigated. In both systems, the XRD patterns indicated the cubic perovskite structure for $0 \leqslant x \leqslant \sim 0.5$ and the orthorhombic perovskite structure for $x = 0.8$ and 1.0. The XRD pattern of $x = 0.6$ sample consists of superposition of the cubic and orthorhombic patterns indicating the two-phase coexisting region. The temperature dependence of electrical resistivity, ρ measured for the both systems showed metallic nature for the cubic perovskite region semiconducting or insulating nature for the orthorhombic region. The $SrCoO_3$ ($x = 0$) compound exhibited ferromagnetism with Curie temperature, $T_c = 266$ K. For the $Sr_{1-x}Y_xCoO_3$ system, T_c increased slightly to 275 K at $x = 0.1$, then decreased rapidly to ~60 K for $x = 0.6$. The magnetic data suggested mixing of the low-spin and intermediate-spin states of the Co ion for the ferromagnetic region. But possibility of itinerant-electron ferromagnetism picture could not be ruled out. The orthorhombic perovskite $YCoO_3$ showed non-magnetic behavior indicating the low-spin state of the Co^{3+} ion. Quite similar results were obtained on the magnetism of the $Sr_{1-x}Ho_xCoO_3$ system.

Acknowledgments

The author (SB) is thankful to NIMS for awarding the NIMS-Post Doctoral Fellowship. This study was partially supported by Grants-in-Aid for Scientific Research from the Japan Society for the Promotion of Science (16076209, 16340111).

References

[1] H. Watanabe, J. Phys. Soc. Jpn. 12 (1957) 515.
[2] H. Watanabe, T. Takeda, in: Y. Hoshino, et al. (Eds.), Proceedings of the International Conference on Ferrites, Kyoto, July 1970, University Park Press, Baltimore, MD, 1971, p. 588.
[3] T. Takeda, Y. Yamaguchi, H. Watanabe, J. Phys. Soc. Jpn. 34 (1972) 970.
[4] J.C. Grenier, S. Ghobane, G. Demazeau, M. Pouchard, P. Hagenmuller, Mater. Res. Bull. 14 (1979) 831.
[5] Y. Takeda, R. Kanno, O. Yamamoto, M. Takano, Y. Bando, Z. Anorg. Allg. Chem. 540–541 (1986) 259.
[6] H. Taguchi, M. Shimada, F. Kanamaru, M. Koizumi, Y. Takeda, J. Solid State Chem. 18 (1976) 299.
[7] H. Taguchi, M. Shimada, M. Koizumi, J. Solid State Chem. 29 (1979) 221.
[8] T. Takeda, H. Watanabe, J. Phys. Soc. Jpn. 33 (1972) 973.
[9] D. Bahadur, S. Kollali, C.N.R. Rao, M.J. Patni, C.M. Srivastava, J. Phys. Chem. Solids 40 (1979) 981.
[10] P.D. Battle, M.A. Green, J. Lago, A. Mihut, M.J. Rosseinsky, L.E. Spring, J. Singleton, J.F. Vente, Chem. Commun. (1998) 987.
[11] H. Taguchi, M. Shimada, M. Koizumi, Mater. Res. Bull. 15 (1980) 165.
[12] R.H. Potze, G.A. Sawatzky, M. Abbate, Phys. Rev. B 51 (1995) 11501.
[13] M. Zhuang, W. Zhang, A. Hu, N. Ming, Phys. Rev. B 57 (1998) 13655.
[14] S. Mukherjee, R. Ranganathan, P.S. Anilkumar, P.A. Joy, Phys. Rev. B 54 (1996) 9267.
[15] P.L. Kuhns, M.J.R. Hoch, W.G. Moulton, A.P. Reyes, J. Wu, C. Leighton, Phys. Rev. Lett. 91 (2003) 127202.
[16] G.H. Jonker, J.H. van Santent, Physica (Amsterdam) 19 (1953) 120.
[17] M.A. Señarís-Rodríguez, J.B. Goodenough, J. Solid State Chem. 118 (1995) 323.
[18] R. Caciuffo, D. Rinaldi, G. Barucca, J. Mira, J. Rivas, M.A. Señarís-Rodríguez, P.G. Radaelli, D. Fiorani, J.B. Goodenough, Phys. Rev. B 59 (1999) 1068.
[19] M. Itoh, I. Natori, S. Kubota, M. Motoya, J. Phys. Soc. Jpn. 63 (1994) 1486.
[20] P.S. Anil-Kumar, P.A. Joy, S.K. Date, J. Phys.: Condens. Matter 10 (1998) L487.
[21] R.L. Withers, M. James, D.J. Goossens, J. Solid State Chem. 174 (2003) 198.
[22] S.Y. Istomin, J. Grins, G. Svensson, O.A. Drozhzhin, V.L. Kozhevnikov, E.V. Antipov, J.P. Attfield, Chem. Mater. 15 (2003) 4012.
[23] S.Y. Istomin, O.A. Drozhzhin, G. Svensson, E.V. Antipov, Solid State Sci. 6 (2004) 539.
[24] M. James, D. Cassidy, D.J. Goossens, R.L. Withers, J. Solid State Chem. 177 (2004) 1886.
[25] D.J. Goossens, K.F. Wilson, M. James, A.J. Studer, X.L. Wang, Phys. Rev. B 69 (2004) 134411.
[26] A. Maignan, S. Hébert, V. Caignaert, V. Pralong, D. Pelloquin, J. Solid State Chem. 178 (2005) 868.
[27] W. Kobayashi, S. Ishiwata, I. Terasaki, M. Takano, I. Grigoraviciute, H. Yamauchi, M. Karppinen, Phys. Rev. B 72 (2005) 104408.
[28] S. Balamurugan, M. Xu, E. Takayama-Muromachi, J. Solid State Chem. 178 (2005) 3441.
[29] G. Demazeau, M. Pouchard, E.P. Hagenmuller, J. Solid State Chem. 9 (1974) 202.
[30] A. Mehta, R. Berliner, R.W. Smith, J. Solid State Chem. 130 (1997) 192.
[31] O.S. Buassi-Monroy, C.C. Luhrs, A. Chavez-Chavez, C.R. Michel, Mater. Lett. 58 (2004) 716.
[32] V.G. Bhide, D.S. Rajoria, Y.S. Reddy, G. Rama Rao, C.N.R. Rao, Phys. Rev. B 8 (1973) 5028.
[33] S. Balamurugan, K. Yamaura, E. Takayama-Muromachi, unpublished.
[34] C. Zener, Phys. Rev. 81 (1951) 440.
[35] P. Rhodes, E.P. Wohlfarth, Proc. Roy. Soc. 273 (1963) 247.